Available online at www.sciencedirect.com

ScienceDirect

IFAC Papers Online CONFERENCE PAPER ARCHIVE

IFAC PapersOnLine 55-20 (2022) 546–551

Multi-objective optimal control for energy extraction and lifetime maximisation in dielectric elastomer wave energy converters ⋆

Matthias K. Hoffmann * **Giacomo Moretti** **
Gianluca Rizzello ** **Kathrin Flaßkamp** *

* *Systems Modeling and Simulation,*
(e-mail: {matthias.hoffmann, kathrin.flasskamp}@uni-saarland.de)
** *Intelligent Material Systems Lab,*
(e-mail: {giacomo.moretti, gianluca.rizzello}@imsl.uni-saarland.de)
* *and* ** *from Saarland University, Saarbrücken, Germany.*

Abstract: In this paper, we model the multi-objective optimisation problem for maximising the energetic performance while minimising the damage accumulation in ocean wave energy converters based on dielectric elastomer generators (DEGs). DEGs are electrostatic smart-material-based transducers that are cheaper, lighter, and more adaptable to the marine environment than conventional power take-off systems. Because DEGs are prone to electrical breakdown upon cyclic loading, identifying trade-offs between achievable performance and lifetime is currently a crucial research question. Based on some assumptions on the system layout and material properties, and using the methods of Pareto optimisation, we prove that a suitably chosen control strategy can potentially achievez a dramatic reduction in the accumulated damage at the expense of a small reduction in the harvested energy. We further compare the Pareto optimal control solutions with commonly used control heuristics for DEGs, showing that optimal control can provide a reduction in the accumulated damage while preserving (or even improving) the energy performance.

Keywords: Optimal Control, Dielectric Elastomer Generators, Wave Energy, Multi-Objective Optimization, Non-Linear Optimization, Pareto optimization

1. INTRODUCTION

Although ocean wave energy is one of the most abundant and highly concentrated forms of renewable energy, to date high technological complexity and capital costs have prevented wave energy converter (WEC) technologies from reaching the market (Pecher and Kofoed (2017)). A potentially disruptive solution in this field is represented by the so-called dielectric elastomer generators (DEGs). DEGs are lightweight polymeric generators that enable direct-drive mechanical-to-electrical power conversion, and provide a potentially cheaper and simpler solution than conventional power take-off systems for wave energy (Moretti et al. (2020)). Whereas, in the last decade, numerical analyses and wave tank tests have uncovered the potential of this technology, major technical unknowns related to lifetime and long-term reliability of DEG power take-off systems still exist. Despite the observation, by Chen et al. (2019a), that electrical breakdown is the main cause of failure for DEG, the application of large electric fields is key if large energy conversion densities are sought. Identifying suitable driving strategies which are able to realise a trade-off between energetic performance and lifetime is thus key for the success of DEG-based energy harvesting applications.

In this work, we use Pareto optimisation to analyse the relation between energy scavenged from and damage accumulated by a DEG-WEC device. Building upon a DEG-WEC model, we formulate a multi-objective dynamic programming problem seeking the optimisation of the energy harvested by the DEG, and the minimisation of a damage cost accounting for the DEG cyclic electrical loading. The Pareto fronts are numerically computed to include solutions for different mutual weightings of the costs. Moreover, we parameterise the problem by sea state factors. Analyzing the numerical solutions revealed qualitatively different trends in the Pareto-optimal profiles of the DEG driving voltage. We then compare such optimal controls with heuristic bang-bang controllers used in literature, and we show that the optimal control allows converting larger amounts of wave energy, even in the presence of safer lower electric fields.

In contrast with previous articles on optimal control of WECs for maximum power conversion (see Faedo et al. (2017)), this is the first work that deals monolithically with energetic performance and lifetime optimisation via Pareto optimisation. Compared with previous works on dynamic programming with DEG-WEC systems (Rosati Papini

⋆ GM received funding from the European Union's Horizon 2020 research and innovation programme under the Marie Skłodowska-Curie grant agreement No 893674 (DEtune).

10.1016/j.ifacol.2022.09.152

et al. (2018)), moreover, this work introduces a more realistic recast of the energetic cost function for the DEG, which explicitly accounts for the effect of electrical losses in the dielectric.

2. MODEL AND PROBLEM STATEMENT

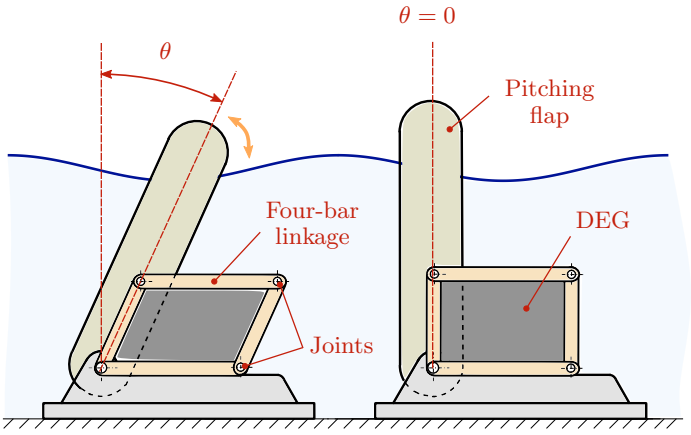

Fig. 1. Pitching flap WEC with parallelogram DEG: generic position (left); and vertical equilibrium position (right)

2.1 Background

We investigate a WEC layout known as wave surge converter (see, e.g., Whittaker and Folley (2012)). The device (Fig. 1) consists of a bottom-hinged flap (or paddle) put into oscillation by the waves. Here we assume that the surge holds a parallelogram DEG as the direct-drive electrical power converter (see Moretti et al. (2014)). The parallelogram DEG consists of a stack of stretchable elastomeric dielectric membranes, covered by compliant electrodes and electrically connected in parallel, attached through their perimeter to the links of a four-bar linkage with two couples of parallel links (namely, a parallelogram mechanism). The parallelogram DEG provides the flap with a controllable torque. Applying a voltage on the electrodes generates an electrostatically-induced torque that that pushes the flap towards position $\theta = 0$.

The system has one kinematic degree of freedom, described by the angle θ between the flap and the vertical. Assuming that the DEG membrane is equally pre-stretched in the planar directions, $\theta = 0$ (see Fig. 1) is an equilibrium position for the system.

Cyclically controlling and optimising the profile of the applied voltage as a function of the wave excitation and the system dynamics allows maximising the power converted by the DEG in different sea states (see Rosati Papini et al. (2018)). On the other hand, the electric field generated upon voltage application creates a damage on the dielectric material, which accumulates in time, and ultimately leads to the system failure (Chen et al. (2019a)). Whereas optimising the energetic performance potentially demands for large electric fields being applied on the material, lifetime considerations push towards work regimes with lower electric fields.

2.2 Model

Based on our previous work (Moretti et al. (2014)), we describe the dynamics of the surge in terms of the pitching flap equation of motion, plus an additional dynamics describing in a simplified linear manner the wave loads generated by the waves radiated from the flap. Since the electrostatic forces generated by a DEG are proportional to the square of the voltage, we hereby call u (namely, the system input) the square of the applied voltage v ($u = v^2$) and cast the wave surge dynamics as follows:

$$\begin{bmatrix}\dot{\theta}\\ \dot{\vartheta}\\ \dot{z}\end{bmatrix} = \begin{bmatrix}0 & 1 & 0^{1\times n}\\ -I_h^{-1}K_h & -I_h^{-1}B_h & -I_h^{-1}C_r\\ 0^{n\times 1} & B_r & A_r\end{bmatrix}\begin{bmatrix}\theta\\ \vartheta\\ z\end{bmatrix} + \\ + \begin{bmatrix}0\\ I_h^{-1}\\ 0^{n\times 1}\end{bmatrix}(d - C_0\theta u)\,, \tag{1}$$

where $\vartheta = \dot{\theta}$ is the flap angular velocity, and $z \in \mathbb{R}^n$ is an $n-$dimensional state vector describing wave radiation (Yu and Falnes (1995)); I_h, B_h and K_h are the flap inertia, a damping coefficient rendering the hydrodynamic losses, and a stiffness coefficient rendering the restoring loads due to the hydrostatic forces and the joints torsional stiffness; $A_r \in \mathbb{R}^{n\times n}$, $B_r \in \mathbb{R}^{n\times 1}$ and $C_r \in \mathbb{R}^{1\times n}$ are matrices describing a passive linear system, and are related to the wave radiation problem; $d = d(t)$ is a time-dependent wave excitation torque due to the incident waves).

The last term in (1) describes the controllable torque of the DEG. Electrically, we model the DEG as a variable capacitor with capacitance $C \approx (1-\theta^2)C_0$ (C_0 being the DEG capacitance at $\theta = 0$; $1-\theta^2$ coming from Taylor second order expansion of the DEG capacitance), and a resistor (assumed constant with resistance R_0) that accounts for the leakage current loss in the elastomeric dielectric. As demonstrated by Moretti et al. (2014), the torque of a parallelogram DEG can be approximated as a single electrostatic term, since elastic contributions from the elastomer are negligible. Such electrostatic torque is proportional to the derivative of the capacitance (i.e., $\mathrm{d}C/\mathrm{d}\theta \approx -2C_0\theta$), and the electric input u. Because of the DEG contribution, dynamics (1) are non-linear.

The maximum electrostatic torque that the DEG can generate is upper bounded by the ultimate breakdown strength of the dielectric elastomer, which sets a static upper limit to u:

$$u \leq (E_{bd}h_l)^2/\cos^2(\theta), \tag{2}$$

where E_{bd} is the ultimate breakdown electric field of the elastomer, and h_l the thickness (at $\theta = 0$) of the DEG layers.

With the aim of highlighting relevant trends in the system response, here we consider sinusoidal wave excitation d:

$$d(t) = 0.5H_w\Gamma(f_w)\sin(2\pi f_w t) \tag{3}$$

where t is time, H_w and f_w are the crest-to-trough height and frequency of a target regular wave, and $\Gamma(f_w)$ is a hydrodynamic frequency-dependent excitation coefficient.

2.3 Heuristic control law

Driving strategies for DEGs used in practical studies usually rely on simple control heuristics. An example of

control heuristic proposed by Moretti et al. (2014) for the surge WEC is as follows:

$$\begin{cases} u = U_{\text{on}}, & \text{if } \theta\dot{\theta} \geq 0 \\ u = 0, & \text{if } \theta\dot{\theta} < 0 \end{cases} \tag{4}$$

where U_{on} is a constant. According to (4), a voltage is applied on the DEG only during the phases in which the electrodes surface (and, hence, the capacitance) decreases ($\theta\dot{\theta} \geq 0$), whereas the DEG is allowed to deform passively ($u = 0$) while its capacitance is increasing. It has been proven that this heuristic ensures that a net amount of electrical energy is positively generated during a wave period. Moreover, the application of heuristic (4) does not require a-priori knowledge of the excitation, as it just relies on measurements of the system's state (θ and $\dot{\theta}$).
In fact, (4) is a sub-optimal control, which does not allow extracting the maximum available amount of energy, and makes use of a single parameter (namely, U_{on}) as the only available degree of freedom to realise a trade-off between energy performance and lifetime.

2.4 Optimal control

With the aim of overcoming the limitations of heuristic control (4), we formulate a multi-objective optimisation problem bearing the optimal input profile $u(t)$ as the unknown, and the following objective functions: 1) the electrical energy scavenged by the DEG; and 2) a measure of the electrical damage accumulated by the material during operating.

The first cost function equals the electrical energy converted by the DEG in a time window of length t_f (with reversed sign), which reads as follows:

$$J_1 = \Psi(t_f) - \Psi(0) + \int_0^{t_f} \left(B_h\dot{\theta}^2 + z^\intercal S_r z + \frac{u}{R_0} - d\dot{\theta} \right) \mathrm{d}t$$
$$\text{with } \Psi = \frac{1}{2} I_h\dot{\theta}^2 + \frac{1}{2} K_h\theta^2 + \frac{1}{2} z^\intercal Q_r z + \frac{1}{2} C_0 \left(1 - \theta^2\right) u \tag{5}$$

Here, Ψ is the system storage function, which includes kinetic, potential, electrostatic, and hydrodynamic energy contributions, whereas the terms in the integral function represent dissipations due to viscous losses, hydrodynamic losses, electrical losses in the DEG, and the power input due to the incident wave respectively. Symmetric matrices Q_r and S_r render the losses and the storage function of the radiated waves, and are calculated from $A_r,\ B_r,\ C_r$ such that:

$$\begin{aligned} S_r = -0.5\left(A_r^\intercal Q_r + Q_r A_r\right) \succ 0, \\ Q_r \succ 0,\ Q_r B_r = C_r^\intercal, \end{aligned} \tag{6}$$

where $\succ 0$ denotes positive definiteness. The existence of symmetric matrices Q_r and S_r which satisfy (6) is guaranteed by the passivity of system (A_r, B_r, C_r), see Duan and Yu (2013).

The second cost penalises the application of large electric fields, which statistically cause damage to accumulate in the DEG (Chen et al. (2019a)). Based on experimental evidence (Dissado and Fothergill (1992)), we assume that damage only accumulates when the electric field surpasses a certain threshold value E_{th}, and cast the associated cost function as follows:

$$J_2 = \alpha \int_0^{t_f} \left(\max\{\cos^2(\theta)u - E_{th}^2 h_l^2, 0\}\right)^{n_d} \mathrm{d}t, \tag{7}$$

where n_d is an experimental parameter, and α is a suitable normalisation factor which renders J_2 dimensionless. We remark that (7) is a heuristic cost, used here with the aim of capturing, in a simple manner, a threshold damage accumulation process.

Combining costs (5) and (7) with dynamics (1) and constraint (2) provides a multi-objective optimization (MOO) problem in u.

Problem 1. The constrained continuous-time multi-objective Optimal Control Problem (OCP) of the system's energetic output (J_1) and damage cost (J_2) is given by

$$\begin{aligned} &\underset{u(t)}{\text{minimize}} \quad (J_1, J_2) \\ &\text{subject to dynamics (1)} \\ &\qquad 0 \leq \cos^2(\theta)u \leq (E_{bd} h_l)^2. \end{aligned} \tag{8}$$

Notice that the last constraint in (8) requires u to be positive since we have $u = V^2$.

3. METHODS

In this section, we first present the numerical approach for solving the OCP. Second, the methods of MOO used in this work are described.

3.1 Discretised Optimal Control Problem formulation

Equation (8) describes an OCP constrained by the dynamics (1). Evaluations of the cost functions are handled by including their integrands into the system dynamics (i.e. transformation to Mayer form), resulting in the new augmented state $\xi = [\theta\ \vartheta\ z^\intercal\ \Upsilon_1\ \Upsilon_2]^\intercal$ with the additional dynamics

$$\begin{aligned} \dot{\Upsilon}_1 &= B_h\dot{\theta}^2 + z^\intercal S_r z + \frac{u}{R_0} - d\dot{\theta} \\ \dot{\Upsilon}_2 &= \left(\max\{\cos^2(\theta)u - E_{th}^2 h_l^2, 0\}\right)^{n_d}. \end{aligned} \tag{9}$$

To tackle the problem numerically, we discretise the augmented dynamics (by means of integrator functions), so as to resort to a finite-dimensional minimisation problem. Denoting Δ the constant discretisation time-step, the time t corresponding to time-step $k \in [0, N-1]$ is $t = k \cdot \Delta$, where N denotes the number of time steps the system is predicted into the future. We then indicate with $\xi[k]$ and $u[k]$ the evaluation of the state and the input at the k-th time-step. The initial condition of the system is denoted by $\xi[k = 0]$. We use the classic Runge-Kutta-Method of order 4 (RK4) as an (explicit) integrator, assuming a first-order hold behaviour for u and d. The dynamics in (8) are discretised and incorporated in the minimisation problem as a set of equality constraints in the form

$$\xi[k+1] = F_{RK4}(\xi[k], u[k], u[k+1])\ \forall\ k \in [0, N-2], \tag{10}$$

where $F_{RK4}(\xi[k], u[k], u[k+1])$ is an integrator function describing the time-step-wise system evolution, calculated from (8). Then $J_1 \approx \Upsilon_1[N-1]$ and $J_2 \approx \Upsilon_2[N-1]$.

3.2 Multi-objective Optimization

We tackle the multi-objective problem (8) by transforming the vector cost function into a scalar function, hence en-

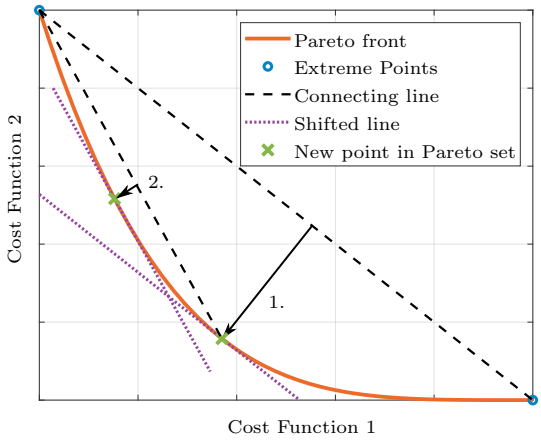

Fig. 2. Qualitative illustration of the first steps of the AWDS algorithm.

abling the use of single-objective optimization techniques (Marler and Arora (2004)).

In this work, we use the weighted sum method as the scalarization method. Let us denote $w_1 J_1 + w_2 J_2 = c$ an arbitrary line in the objective space, with the left-hand side being the weighted sum and c a constant. The units of the weights w_1 and w_2 (for J_1 and J_2 respectively) are such that the resulting weighted sum is dimensionless. Geometrically, minimising the weighted sum is equivalent to decreasing c, and thus shifting the line as far as possible into the direction where both costs decrease, while still maintaining at least one feasible point.

We generate a Pareto set with evenly distributed points through an iterative procedure based on the Adaptive Weight Determination Scheme (AWDS) algorithm by Ryu and Min (2019). For two objectives, the two extreme points of the Pareto front are first calculated by using two different combinations (w_1, w_2), with $w_1 \gg w_2$ and $w_1 \ll w_2$ respectively. At each iteration, the straight line connecting two Pareto points is calculated, and the coefficients of J_1 and J_2 in the line equation are then used as the new weights for the weighted sum method. This solution produces a new Pareto optimal point in between the parent points. This algorithm is repeated with all combinations of parent points and the new points that they originate, until a breaking condition is fulfilled. Fig. 2 shows the first two steps of the algorithm.

3.3 Conditioning of the problem

To render the numerical values of the two costs on the same order of magnitude, cost J_1 is numerically expressed in MW (i.e., the dimensional unit of w_1 is MW^{-1}, whereas w_2 is dimensionless).

To prevent numerical ill-conditioning, u is first rescaled from V^2 to kV^2. Problem 1 is then simplified by using the approximation $\cos^2(\theta) \approx 1$ in the expression of J_2 and in the inequality constraint. This is a conservative approximation, such that the resulting inequality constraint is a stricter version of (2), and cost J_2 is larger or equal than that defined by the expression in (7).

With these assumptions, Problem 1 can be recast as the following minimisation problem.

Problem 2. The constrained discrete-time minimisation problem with scalarised multi-objective cost is given by

$$\begin{aligned} \underset{u[0],\ldots,u[N-1]}{\text{minimize}} \quad & w_1 J_1 + w_2 J_2 \\ \text{subject to } & \xi[k+1] = F_{RK4}(\xi[k], u[k], u[k+1]) \\ & \forall\ k \in [0, N-2], \\ & 0 \le u[k] \le (E_{bd} h_l)^2,\ \forall\ k \in [0, N-1]. \end{aligned} \tag{11}$$

4. NUMERICAL RESULTS

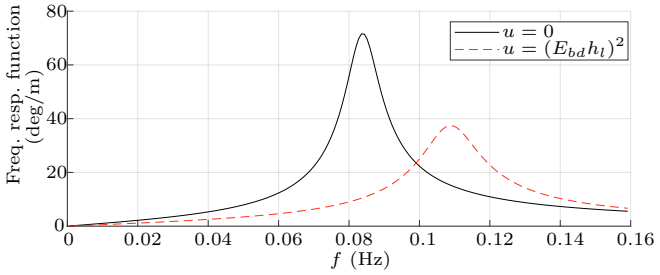

Fig. 3. Frequency response function of the system at two constant fixed values of the input.

We present a numerical case study based on the wave surge design envisaged by Moretti et al. (2014), which make reference to a hypothetical large-scale surge WEC with parallelogram DEG made of natural rubber. The parameters of the system are summarised in Tab. 1. The same hydrodynamic parameters (A_r, B_r, C_r, $\Gamma(f)$) as in the reference article are used here. Although accurate data on the stochastic damage accumulation in rubber are sparse, for the aim of this analysis approximate data have been extrapolated from preliminary studies on electrical fatigue in dielectric elastomers (Chen et al. (2019b,a)).

The linear frequency response function of the system (i.e., the angular oscillation amplitude per unit wave height at different frequencies) obtained by setting u constant is shown in Fig. 3. The frequency response is calculated at the two limit values of u, i.e. $u = 0$ and $u = (E_{bd} h_l)^2$. The peak in the frequency responses curve corresponds to the natural pitching frequency of the surge, which is $f_w \simeq 0.084$ Hz (i.e., a resonance period of 11.9 s) at $u = 0$, and $f_w \simeq 0.11$ Hz (i.e., resonance period of 9.1 s) at the maximum allowed input, because the electrostatic loads cause an increase in the system stiffness (see (1)).

Table 1. Case study parameters

Param.	Value	Param.	Value
I_h	$2.3 \cdot 10^7$ kg·m^2	h_l	275 μm
C_h	$2 \cdot 10^6$ N·m·s	E_{bd}	120 kV/mm
K_h	$1.7 \cdot 10^7$ N·m	E_{th}	80 kV/mm
C_0	139 mF	n_d	2
R_0	3.4 kΩ	α	10^{-6} kV^{-4}s^{-1}

In the following, we present numerical solutions to Problem 2 in (11) produced in MATLAB using the software library IPOPT by Wächter and Biegler (2006) as the solver, and CasADi by Andersson et al. (2019) to conveniently formulate the problem. Each of the simulations and optimizations were run on a time horizon of $T = 50$ s and a sampling time $\Delta = 0.1$ s, starting from the system steady state oscillation, calculated at $u = 0$. A fixed wave height $H = 2$ m is used in the presented examples.

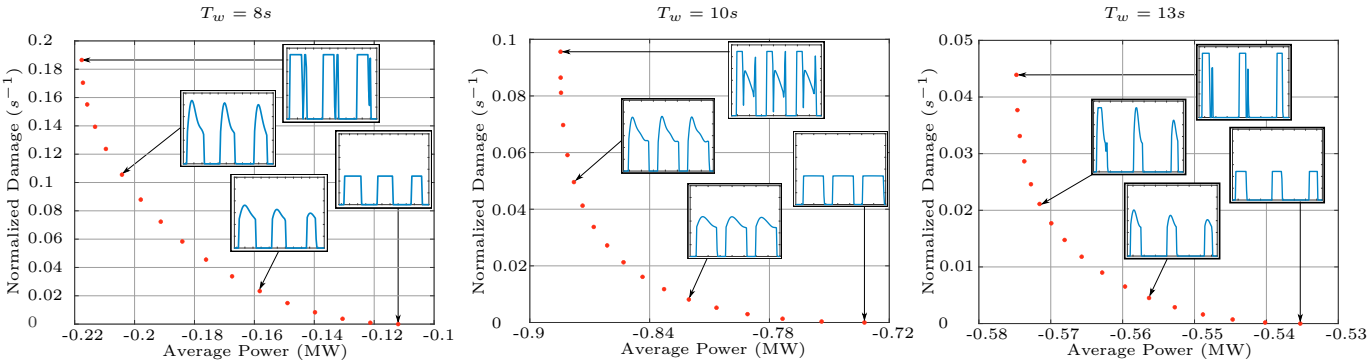

Fig. 4. Three Pareto fronts relative to different wave periods, with representative optimal steady-state solutions for u.

Fig. 4 shows three Pareto sets for sea states with wave periods $T_w = 8,\ 10,\ 13$ s. The axes report the average rates of produced energy and accumulated damage (i.e., the mean values of the cost per unit time). Each point of the Pareto sets is obtained by choosing different combinations of weights w_1 and w_2 for J_1 and J_2 respectively. The resulting Pareto fronts are convex and their shape suggests that a meaningful exploitable trade-off between the two objectives can be realised. For $T_w = 8$ s the accumulated damage can be halved by reducing the expected energy output by only 10 %. For $T_w = 10,\ 13$ s, the same reduction in damage can be achieved with a energy loss of less than 1 %, highlighting the potential of including the damage cost function into the design of an optimal control.

Examples of the steady-state trend of u for some significant Pareto optimal points on each of the sets are shown in the insets. The optimal profiles of u are characterised by intervals in which the DEG deforms passively ($u = 0$) and intervals in which a voltage is actively applied. The optimal control profiles corresponding to the same combination of weights significantly vary from one wave period to another. For wave periods close to the range of the natural periods of the system (see Fig. 3), the controller adjusts the duration of the phases during which a voltage is applied on the DEG so as to tune the system with the incoming waves. In particular, for $T_w = 10$ s, the controller keeps the DEG activated ($u > 0$) for a large fraction of the overall wave period, so as to increase the system stiffness and match its (average) natural period with the wave frequency (see Fig. 3). Dually, for $T_w = 13$ s (i.e., slightly below the system natural frequency at $u = 0$ - see Fig. 3), the controller keeps the DEG active for a shorter amount of time, hence preventing its natural frequency to become excessively larger than the wave frequency. For $T_w = 8$ s, in contrast, the system is considerably off the resonance range. In this case, the controller limits the amount of time during which $u > 0$, so as to limit the amount of damping applied by the DEG on the surge.

The average power extracted in based on a given combination of weights is maximum for T_w =10 s, which lies in between the minimum and maximum natural frequency that the system can achieve (Fig. 3), and it is minimum for $T_w = 8$ s, i.e. when the system is off-resonance.

Interestingly, the optimal profiles of u relative to the case $w_1 \gg w_2$ change drastically based on the sea-state. In particular, for $T_w = 8, /13$ s, the controller approximately follows a bang-bang behaviour, in which the control u reaches the limit value $E_{bd}^2 h_l^2$. For $T_w = 10$ s, i.e., the sea state where the DEG can extract maximum energy, a more complex profile of the activation voltage is pursued.

With reference to a sea state with $T_w = 10$ s, we hereby compare heuristic control law (4) described in Sect. 2.3 with the optimal control solutions. To this end, Fig. 5 compares the optimal profiles of the control u and the angle θ achieved with two different combinations of the weights (w_1, w_2) with the heuristic control described in Sect. 2.3. The plots on the left compare the optimum control, obtained using $w_1 \gg w_2$, with heuristic control (4) and $U_{\text{on}} = (E_{bd} h_l)^2$. In this case, the optimal control produces an average power of 0.88 MW and damages the DEG with an average rate ($\dot{J}_2$) of approximately $0.10\,\text{s}^{-1}$, whereas the heuristic controller's power generation is 0.45 MW with damage costs of $0.17\,\text{s}^{-1}$. In practice, the optimum control finds a strategy to reduce the accumulated damage by keeping the voltage on the DEG at the breakdown value for a shorter amount of time, while achieving larger power conversion by keeping the voltage on a longer total amount of time. Both the optimal and the heuristic control quickly switch on the voltage at the same time instant (when the DEG capacitance is maximum), but they use different phases for the voltage switch-off. The plots on the right in Fig. 5 compare the optimal solution obtained for $w_1 \ll w_2$ with heuristic controller (4) with $U_{\text{on}} = (E_{th} h_l)^2$. In both cases, the control has a bang-bang behaviour with the voltage upper-bounded by the damage accumulation threshold, i.e., the DEG does not accumulate damage. The switch-on and switch-off instants for the voltage are different in the two cases, with the optimum controller keeping the DEG electrically active for a longer amount of time. As a result, the optimal controller leads to an average generated power of 0.73 MW, which compares with a power of 0.39 MW generated by the heuristic controller.

5. CONCLUSION

In conclusion, the present work presents a framework for the identification of optimal controllers for WECs based on DEGs. Multi-objective optimisation is here proposed as a tool to realise a trade-off between the energy performance of the system (i.e., the average power that it can convert) and the damage which is accumulated on the DEG because of cyclic loading. Despite current uncertainties on the nature and the actual extent of the damaging mechanisms in DEGs, based on preliminary qualitative observations, here we assume that damage is accumulated only when the applied electric field surpasses a certain threshold.

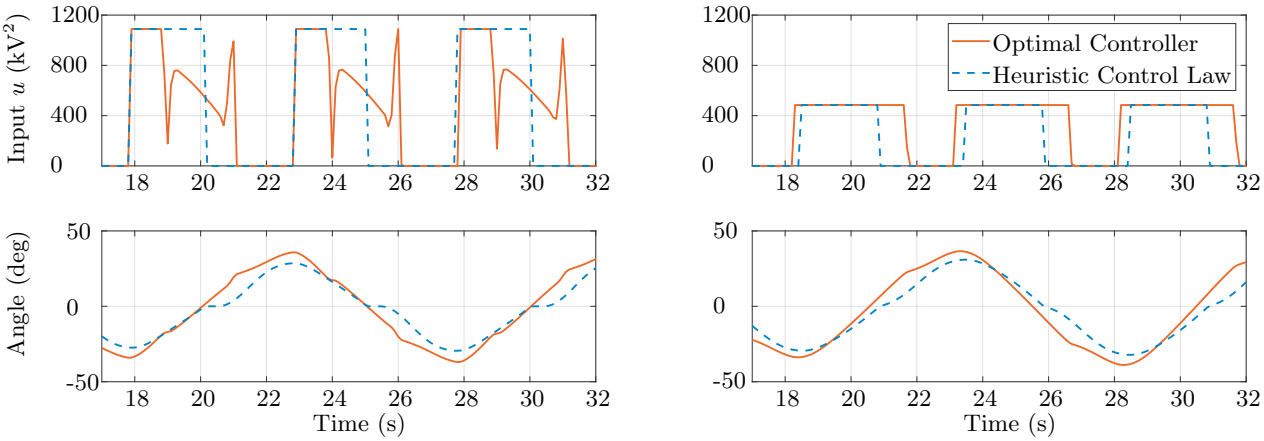

Fig. 5. Comparison of heuristic and optimal controls for $T_w = 10\,\text{s}$ and $H_w = 2$ m. The top row compares the trends of the input u, the bottom row compares the trends of the angular displacement θ. Plots on the left are obtained by setting $w_1 \gg w_2$ in the optimisation problem, and $U_{\text{on}} = (E_{bd} h_l)^2$ in the heuristic control. The optimal control generates an average power of 0.88 MW and a damage accumulation of $0.10\,\text{s}^{-1}$, compared to 0.45 MW and $0.17\,\text{s}^{-1}$ by the heuristic control. Plots on the right column are obtained by setting $w_1 \ll w_2$ in the optimisation problem (0.73 MW), and $U_{\text{on}} = (E_{th} h_l)^2$ in the heuristic control (0.39 MW) with no damage accumulation.

The obtained results show that it is virtually possible to drastically limit damage accumulation with minimal loss of performance compared to a purely energy-oriented optimal control. Compared to heuristic controllers for DEG-WECs based on a prediction-free bang-bang control of the DEG, the optimal control solutions increase the energetic performance, while at the same time reducing the accumulated damage, through an optimised choice of the applied electric field waveforms and peak values. Overall, this study demonstrates the potential behind using multi-objective optimisation to research trade-offs between convertible energy and lifetime in the control of DEG-based WEC. Hence, it motivates further research effort towards the analysis and systematic characterisation of the failure and damage accumulation mechanisms in dielectric elastomers.

REFERENCES

Andersson, J.A.E., Gillis, J., Horn, G., Rawlings, J.B., and Diehl, M. (2019). CasADi – A software framework for nonlinear optimization and optimal control. *Mathematical Programming Computation*, 11(1), 1–36. doi: 10.1007/s12532-018-0139-4.

Chen, Y., Agostini, L., Moretti, G., Berselli, G., Fontana, M., and Vertechy, R. (2019a). Fatigue life performances of silicone elastomer membranes for dielectric elastomer transducers: preliminary results. In *Electroactive Polymer Actuators and Devices (EAPAD) XXI*, volume 10966, 1096616. International Society for Optics and Photonics.

Chen, Y., Agostini, L., Moretti, G., Fontana, M., and Vertechy, R. (2019b). Dielectric elastomer materials for large-strain actuation and energy harvesting: a comparison between styrenic rubber, natural rubber and acrylic elastomer. *Smart Materials and Structures*, 28(11), 114001.

Dissado, L.A. and Fothergill, J.C. (1992). *Electrical degradation and breakdown in polymers*, volume 9. Iet.

Duan, G.R. and Yu, H.H. (2013). *LMIs in control systems: analysis, design and applications*. CRC press.

Faedo, N., Olaya, S., and Ringwood, J.V. (2017). Optimal control, MPC and MPC-like algorithms for wave energy systems: An overview. *IFAC Journal of Systems and Control*, 1, 37–56.

Marler, R.T. and Arora, J.S. (2004). Survey of multi-objective optimization methods for engineering. *Structural and Multidisciplinary Optimization*, 26(6), 369–395. doi:10.1007/s00158-003-0368-6.

Moretti, G., Forehand, D., Vertechy, R., Fontana, M., and Ingram, D. (2014). Modeling of an oscillating wave surge converter with dielectric elastomer power take-off. In *International Conference on Offshore Mechanics and Arctic Engineering*, volume 45530, V09AT09A034. American Society of Mechanical Engineers.

Moretti, G., Rosset, S., Vertechy, R., Anderson, I., and Fontana, M. (2020). A review of dielectric elastomer generator systems. *Advanced Intelligent Systems*, 2(10), 2000125.

Pecher, A. and Kofoed, J.P. (2017). *Handbook of ocean wave energy*. Springer Nature.

Rosati Papini, G.P., Moretti, G., Vertechy, R., and Fontana, M. (2018). Control of an oscillating water column wave energy converter based on dielectric elastomer generator. *Nonlinear Dynamics*, 92(2), 181–202.

Ryu, N. and Min, S. (2019). Multiobjective optimization with an adaptive weight determination scheme using the concept of hyperplane. *International Journal for Numerical Methods in Engineering*, 118(6), 303–319.

Wächter, A. and Biegler, L.T. (2006). On the implementation of an interior-point filter line-search algorithm for large-scale nonlinear programming. *Mathematical programming*, 106(1), 25–57.

Whittaker, T. and Folley, M. (2012). Nearshore oscillating wave surge converters and the development of oyster. *Philosophical Transactions of the Royal Society A: Mathematical, Physical and Engineering Sciences*, 370(1959), 345–364.

Yu, Z. and Falnes, J. (1995). State-space modelling of a vertical cylinder in heave. *Applied Ocean Research*, 17(5), 265–275.